STRUCTURAL AND SPECTRAL STUDY OF BENZO[F]PYRROLO[1,2-a]QUINOLINE WITH POTENTIAL BIOLOGICAL PROPERTIES

G. OANCA, ANTONINA GRITCO TODIRAȘCU, DORINA CREANGĂ[#], DANA DOROHOI

Faculty of Physics, "Alexandru Ioan Cuza" University, 11 Carol I Blvd., Iași, 700506, Romania,
[#]e-mail: dorina.creanga@gmail.com

Abstract. The wide class of quinoline derivatives was much studied due to the various properties that recommend them for applications in chemistry and biomedicine. The present study was focused on such a quinoline derivated molecule that was investigated by computational and spectral methods. Nitrophenyl substituted benzo[f]pyrrolo[1,2-a]quinoline (NPBQ) was studied by a quantum chemical approach using structural and energetic parameters, while experimental spectral data were used to describe its solvatochromic behavior in various solvents. The correlation between the wavenumber in the electronic absorption band recorded in visible range for diluted solutions and the solvent macroscopic parameters – refractive index and relative electric permittivity – was shown based on a solvatochromic theoretical approach. Double linear regression has fitted the experimental data which indicates that both main types of solute-solvent interactions occur in the studied solutions in accordance with the theoretical background. Some specific intermolecular interactions should be also considered to adjust the results of solvatochromic theory application.

Key words: nitrogen organic compound, quantum chemical approach, intermolecular interactions.

INTRODUCTION

Quinolines are nitrogen heterocycle molecules with antiseptic and antipyretic properties, traditionally used as antimalarials or precursors of antimalarial drugs. It was found that antimalarial agents that have been synthesized for decades based on quinolines, like indolo[3,2-c]quinolines – still pharmacologically attractive class of heterocyclic compounds, [22], have to face, however, the development of microbial resistance occurred in recent years [19]. Beside antibacterial action, the antimicrobial activity of some quinoline derivatives was reported [10]; some other quinoline compounds were found to have both antidepressant and antifungal activity [14]; in [20] it was reported the synthesis of a series of nitrogen

Received: December 2015;
in final form January 2016.

ROMANIAN J. BIOPHYS., Vol. 25, No. 4, P. 279–290, BUCHAREST, 2015

heterocycles with potential antidepressant activity as shown when tested in mice. In [3] the authors revealed possible modulators of neuronal activity with quinoline derivatives. Spectral study of organic compounds like quinoline type molecules could be accomplished mainly in diluted solutions. In [4] an ylid type quinoline compound is studied from the viewpoint of solvent effect on the electronic absorption spectrum by applying solvatochromic approach based on the dependence of the wavenumber in the maximum of electronic absorption bands on the solvent refractive index and dielectric constant. In [6] the dependence of the visible range electronic band wavenumber of a benzo[f]quinolinium ylid on solvent nature was analyzed by solvatochromic approach. In [12] most of basic mathematical formalisms proposed for describing solute-solvent interactions using the correlation between spectral shift in electronic spectral bands and various functions on the solvent electro-optical parameters can be found. Thus, the mathematical models proposed by McRae [17], Abe [1], Mataga and Kubota [15], Bakhshiev [2] describe solvatochromic behavior of solute molecules in diluted solutions by quantitative relations between the solute band position in the electronic spectrum and relatively simple functions on the solvent refractive index and dielectric constant. Benzo[f]pyrrolo[1,2-a]quinoline is considered an interesting N-bridgehead heterocyclic system, with structure analogue to the steroid skeleton. In Fig. 1 the structure of the benzo[f]pyrrolo[1,2-a]quinoline derivative studied in this paper is presented.

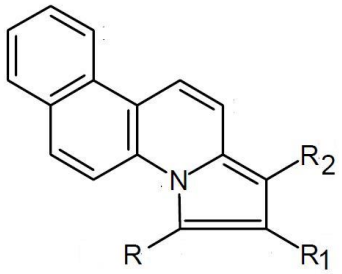

Fig. 1. The structure of studied benzo[f]pyrrolo[1,2-a]quinoline derivative: R = $COC_6H_4NO_2$; $R_1 = R_2 = CO_2CH_3$.

In [9] the authors described the synthesis, by cycloaddition reactions, of benzo[f]pyrrolo[1,2-a]quinoline derivatives, which are interesting due to their chemical and biological properties. Nitrobenzoyl substituted benzo[f]pyrrolo[1,2-a] quinoline is one of such derivatives that was analyzed below using theoretical and experimental methods. The results describing its structural and energetic features as well as the spectral behavior in various solvents are presented in the next chapters.

MATERIALS AND METHODS

QUANTUM CHEMICAL APPROACH

The optimized geometry of the studied compound was determined using DFT B3LYP (Becke, three-parameter, Lee-Yang-Parr) method [13, 21] with 6-31G(d,p) basis set [7]; the atomic charges and electrostatic potential map were also calculated. Further the TD-DFT method [24] was used, with the same level of theory and 6-31G+(d,p) basis set to compute the UV-Vis spectra and the HOMO and LUMO states energy. Gaussian 09 software was used for mathematical simulations [8]; the conjugate gradients algorithm (Polak-Ribier) was employed for the geometry optimization using a convergence limit to 0.0001 kcal/(Å mol). The programs have been running like this: (i) Windows 7 operating system (for HyperChem) on (HP DV6-3034sl) AMD Turion II P520 Dual Core processor of 2.3 GHz and 4GB of RAM and respectively (ii) UBUNTU Server (for Gaussian), using 16 cores on 16-core server, based on Intel Xeon E5-2660 of 2.2 GHz and 63 GB of RAM, at the computer centre of the National Institute of Chemistry, Ljubljana, Slovenia. Also PM3 *ab initio* method with restricted Hartree-Fock (RHF) basis was applied to estimate comparatively the molecular parameters with HyperChem 8.0.10 software [26].

EXPERIMENTAL INVESTIGATION

The solvent arrays listed in Table 1 were used to prepare 10^{-4} M diluted solutions of the NPBQ compound; all those solvents as well as sulfuric acid, used for protonation, were pure reagents acquired from Merck &Co, Inc.

Table 1

The solvents and the functions on the refractive index and the dielectric constant used for spectral data interpretation according to [1]

$f(n)=(n^2-1)/(n^2+2)$	$f(\varepsilon)=(\varepsilon-1)/(\varepsilon+2)$	**Solvent**
0.296	0.3478	O-xylene
0.240	0.5774	N-buthyl acetate
0.266	0.7520	1,2 -Dichlorethane
0.252	0.7945	N-hexyl alcohol
0.219	0.9210	Acetonitrile
0.251	0.9464	Dimethyl sulfoxide

Sulfuric acid aliquot was used for the acidification of studied solutions (up to 1.5 pH) in order to assign spectral bands to main types of electronic transitions.

Spectra recording in the visible and UV range was carried out with UV – 1700 Pharma Spec spectrophotometer from Shimadzu Corporation provided with 1 cm wide quartz cells.

For the statistical interpretation of spectral recorded data the theory proposed by Bakhshiev [2] was applied according to the next formulae.

Eq. (1) is a simplified version of the mathematical relationship proposed in solvatochromic theory, with two main terms, describing dispersive-polarization forces and respectively orientation-induction interactions following the reciprocal influences of solute and solvent molecules:

$$hc\Delta\tilde{\nu} = A(n)\frac{n^2-1}{n^2+2} + B(n)\frac{\varepsilon-1}{\varepsilon+2} \quad (1)$$

where $\Delta\tilde{\nu}$ is the expected spectral shift between the studied electronic absorption spectra (EAS) in isolated molecule (gas) and in the presence of solvent molecules, while n and ε are the solvent macroscopic electro-optic parameters (the refractive index and the dielectric constant). The $A(n)$ term is given by eq. (2):

$$A(n) = (\alpha_g - \alpha_e)\cdot\frac{3}{2a^3}\frac{II'}{I+I'} - \frac{he^2 f}{8\pi m_e \tilde{\nu}_0 a^3} + \frac{2n^2+1}{n^2+2}\frac{\mu_g^2-\mu_e^2}{a^3} \quad (2)$$

where μ_g and μ_e are electric dipole moments in the ground and respectively the excited state, α_g and α_e the electric polarizabilities in the ground and excited states, a is the solute average radius; e and m_e are the electron charge and mass, f is the oscillator strength, I and I' represent solute and the solvent molecules ionizing potentials.

The $B(n)$ term is given by eq. (3) as:

$$B(n) = \frac{2n^2+1}{n^2+2}\cdot\frac{2\mu_g(\mu_g - \mu_e\cos\varphi)}{a^3} \quad (3)$$

where φ is the angle between the two dipole moment vectors.

In the present case the functions $f(\varepsilon) = (\varepsilon - 1)/(\varepsilon + 2)$ and $f(n)=(n^2 - 1)/(n^2 + 2)$ were used to analyze the dependence of $\tilde{\nu}_{exp}$ on the solvent properties.

RESULTS AND DISCUSSION

Quantum chemical DFT simulation generated the energetically optimized geometry of NBPQ molecule (Fig. 2); from the four evidenced conformers, the one chosen for further study was that characterized by minimum total energy at room temperature (Table 2).

From Figs. 2 a, b one can observe the non-planar disposal of the molecule main parts: the benzo[f]quinoline with the addition cycle, the two CO_2CH_3 side

substituents and the $COC_6H_4NO_2$ substituent to the carbon atom near nitrogen; all three atom groups substituting hydrogen ones to the addition cycle are switched out of the main molecular plane. Dipole moment – that has a major role in molecule solubility – was also displayed for the molecule ground state.

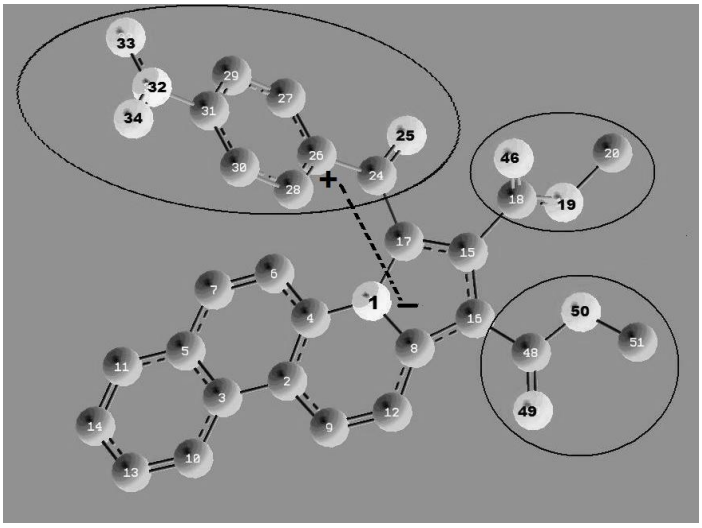

Fig. 2 a. Optimized structure of NPBQ molecule with dipole moment (large dashed line).

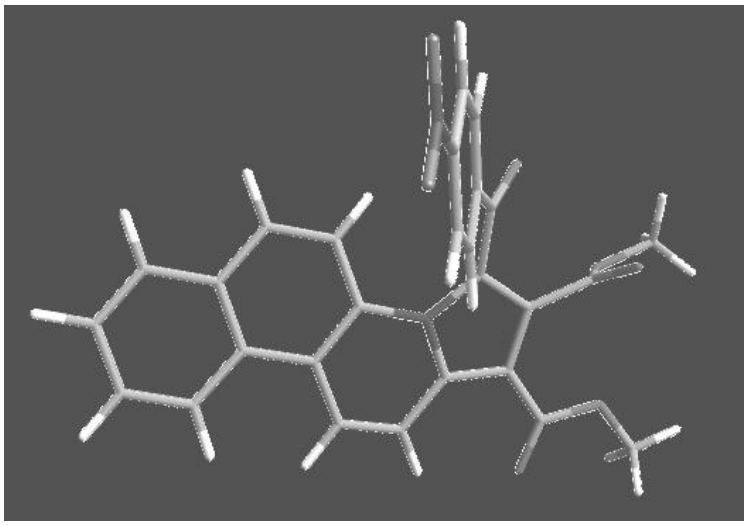

Fig. 2 b. 3-D view of NPBQ optimized geometry.

In Table 2 the results of quantum chemical simulation are presented.

Table 2

Molecular parameters resulted from the two computational approaches

Molecular parameter	DFT B3LYP	*ab initio* PM3
E_{HOMO} (eV)	– 6.17	–8.05
E_{LUMO} (eV)	–3.20	–1.10
Dipole moment (D)	7.95	5.51

HOMO state energy (E_{HOMO}) differs by about 16% between the two approximations while a higher difference of about 66% resulted for LUMO state energy (E_{LUMO}); dipole moment differs by almost 30%.

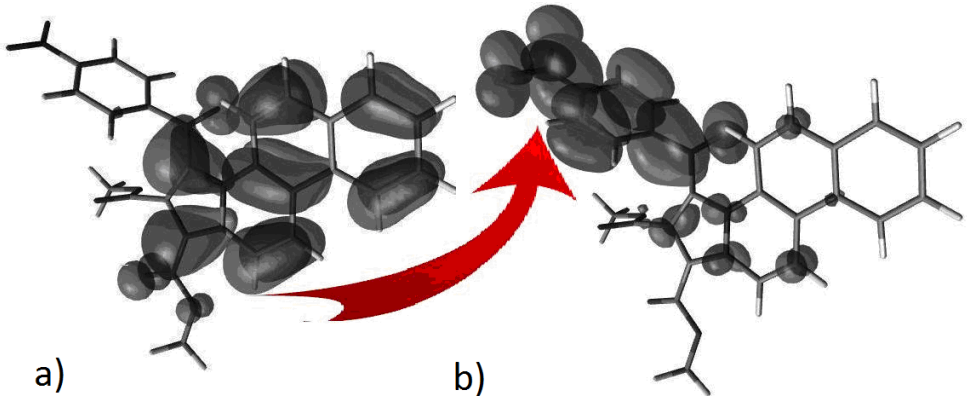

Fig. 3. Frontier electronic orbitals of NPBQ modeled with time dependent DFT/Gaussian: (a) highest occupied molecular orbital (HOMO); (b) lowest unoccupied molecular orbital (LUMO); visualization with Avogadro software [11].

According to Koopman's theorem [5] the value of HOMO energy can be considered the equivalent to–IP (minus ionizing potential) while the value of LUMO energy is a reliable approximation of –EA (minus electron affinity). Literature reports however specify that in case of HOMO energy only the computational method based on Hartree Fock (*ab initio*, PM3) approach [23, 24] could be taken as valuable approach of ionizing potential in some cases – as resulted from experimental measurement for simple molecules. Instead, the following linear correction was proposed: $-HOMO_{corrected} = 1.42 + 1.20\cdot(-HOMO_{calculated})$ for HOMO energy estimated with B3LYP method by DFT approach [23]; no reliable correction could be stated for LUMO state because of high effect of orbital relaxation on eigenvalue of LUMO molecular orbital; more, this seems to be also the case of PM3 *ab initio* LUMO modeling. In the case of our studied molecule, NPBQ, the results of PM3 *ab initio* modeling provided –8.05 eV for HOMO and respectively –1.1 eV for LUMO state, *i.e.* negative values

indicating molecular stability in both ground and excited state; electron affinity may be calculated as EA=1.1 eV while ionizing potential as IP=8.05 eV. DFT modeling with B3LYP functional has led to HOMO energy of – 6.17 eV while linear correction suggested in [24] that was further applied has resulted in –5.98 eV, which is still different compared to the first result (by PM3 approach), but in the limits the calculation method error – of several eV [24]. Thus we might assess the NPBQ ionizing potential as a molecular energetic parameter, best approximated by: $-IP = HOMO_{PM3}$ according to Hartree Fock *ab initio* calculation. In literature report [25] benzo[f]quinoline modeling resulted in HOMO energy of –9.094 eV and LUMO energy of –0.793 eV.

In Fig. 3 the remarkable changes of electronic orbital spatial distribution when passing from HOMO to LUMO orbital are shown; we can see that most of electronic cloud has migrated from the main molecular skeleton (Fig. 3 a) of benzo[f]quinoline with the addition cycle toward the large nitrophenyl ($COC_6H_4NO_2$) substituent. Electrostatic potential map (Fig. 4) of NPBQ ground state shows that around oxygen atoms (colored in light gray) the electronic orbitals are oriented under the main molecular plane while over this plane the large conjugated molecular electron cloud is dominant (in dark gray).

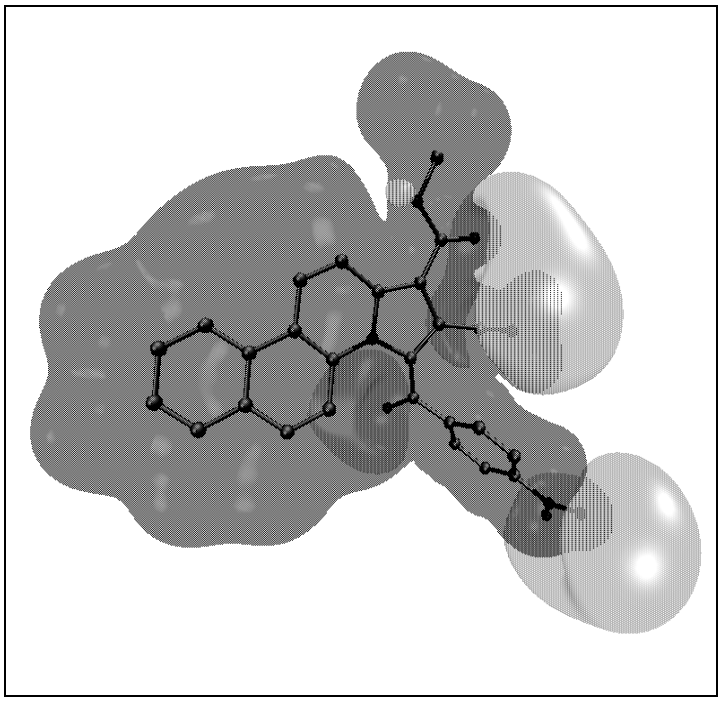

Fig. 4. Electrostatic potential map (colored in light gray – the orbitals disposed under the main molecular plane; colored in dark gray – the orbitals disposed over the main molecular plane).

In Fig. 5, in the recorded EAS, an intense band in the UV range and a group of lower intensity vibronic bands were shaped in visible range.

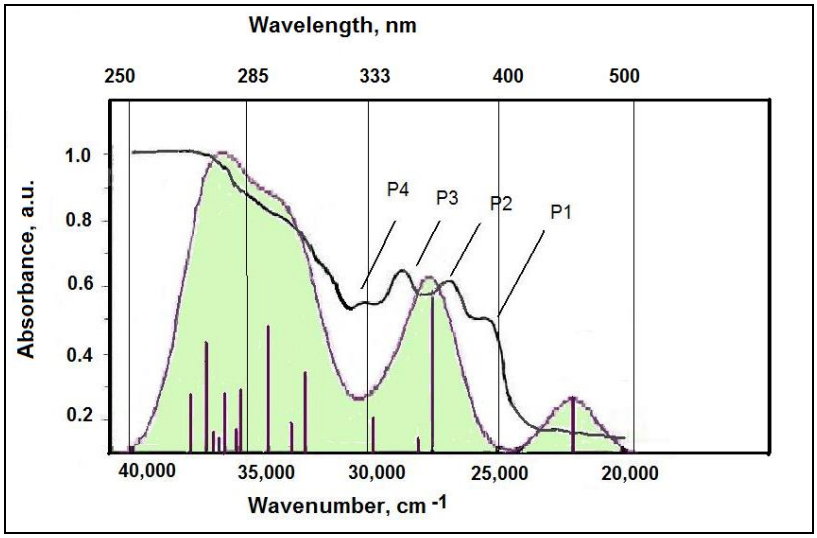

Fig. 5. Normalized EAS of studied NPBQ molecule: simulated EAS for isolated molecule (gas) presented by main absorption transitions (vertical lines) and their approximate envelope; recorded EAS for diluted solution in dimethyl sulfoxide (continuous line with four peaks, P1–P4, in the visible range).

The spectrum recorded in polar solvent (dimethylsulfoxide) appears to have the same basic disposition as the simulated ones but the transition energies are affected by the solvent influence; thus, in the visible range the EAS was shifted hypsochromically and also the near UV band was shifted toward higher wavenumbers.

The differences between the mathematically modeled spectrum and the spectrum recorded in real conditions could be due also to the simplifying hypotheses of the algorithms underlying the modeling software.

SPECTRAL ANALYSIS

The recorded electronic absorption spectra (EAS) of the studied compound are rather stable to the solution protonation (up to 1.5 pH value) with a spectral shift toward blue radiation domain to the increase of solvent polarity, that can be assessed to π –π* transitions [16]. Although nitrogen atom 1 (Fig. 2) has relatively large calculated charge, of –0.72, suggesting possible unbound electron, however, this one seems to be integrated by π conjugation with addition cycle electron cloud

justifying π–π* transitions with possible location on the five atoms heterocycle. The solvatochromism study was carried out on the four band peaks of visible range vibronic band (P1, P2, P3, P4, Fig. 4) due to larger number of solvents with transparency in this range up to 39,000 cm^{-1} and also due to this EAB higher sensitivity to the solvent parameters.

The spectral shifts of the studied peaks reached relatively small values, of several hundreds of cm^{-1} and appeared to change differently to the change of solvent refractive index and/or dielectric constant.

In the case of studied NPBQ molecule the graphical correlations of measured EAS wavenumbers *versus* solvent dielectric constant and refractive index suggested that all known types of universal interaction forces occur between solute molecule and the surrounding solvent.

Thus graphical plots of υ_{exp} *versus* $f(\varepsilon) = (\varepsilon - 1)/(\varepsilon + 2)$ and respectively $f(n)=(n^2 - 1)/(n^2 + 2)$ were analyzed, showing relatively weak linear correlations in both cases (data not presented here) suggesting that neither of the main types of universal forces dominates but rather they have comparable contributions; so that next step of experimental data processing was based on double linear regression approach. Calculated wavenumbers were provided by numerical coefficients generated by statistical processing through double linear regression (with Origin software [18]) according to relations (4) – from the lowest wavenumber band peak P1, to the highest wavenumber one, P4:

$$\tilde{\nu}_{calc} = 25150.8 - 785.9 \cdot f(n) - 4568.6 \cdot f(\varepsilon) \quad (4a)$$

$$\tilde{\nu}_{calc} = 27566.5 + 530.28 \cdot f(n) - 2091.8 \cdot f(\varepsilon) \quad (4b)$$

$$\tilde{\nu}_{calc} = 28718.8 + 192.6 \cdot f(n) - 2052.1 \cdot f(\varepsilon) \quad (4c)$$

$$\tilde{\nu}_{calc} = 33350.8 + 231.4 \cdot f(n) - 3043.8 \cdot f(\varepsilon) \quad (4d)$$

In Fig. 6, the comparison between experimental wavenumbers and those calculated with formula (4) is presented.

Since data points exhibit a certain deviation from the statistical line, we could assume that in the case of the used solvents significant specific interactions also occur that are not described in solvatochromic theories) besides universal ones but causing some evident differences between experimental values of EAB position in the wavenumber scale and the values calculated by considering only universal interaction forces. Hydrogen bonds are most probably present in some solvents where side hydrogen could be attracted toward oxygen atoms (33 and 34, Fig. 2) of

solute molecule nitro group where calculated electric charges were of about – 0.41; or involving oxygen atoms (46 and 49, Fig. 2) from carbonyl groups (with –0.40 and –0.54 electron charges).

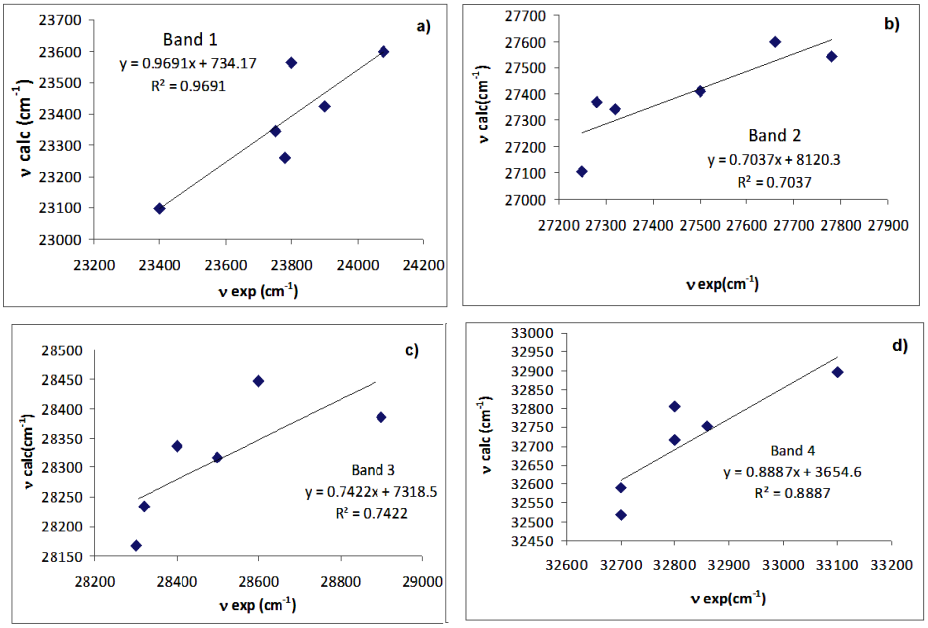

Fig. 6. Comparison of experimental wavenumbers and calculated ones by linear double regression, corresponding to the four analyzed spectral bands (a) P1, (b) P2, (c) P3, (d) P4.

CONCLUSION

N-heterocyle derivate from benzo[f]quinoline with possible chemical features of dyes and possible biological activity was found to be theoretically rather stable – with negative HOMO and LUMO energies; however relatively high dipole moment (7.95 D according to DFT modeling) is favorable to dipole-dipole interaction with polar solvents. N-atom from heterocycle has a significant negative charge (–0.71), as shown by DFT simulation of optimized geometry, but its electron cloud seems to be conjugated with the addition cycle π orbitals, so that specific solvatochromism was observed to the studied electronic absorption π–π* transition. The present study could be useful in practical manipulation of N-heterocycle solutions in various solvents in fabrication process or for chromatographic analysis.

REFERENCES

1. ABE, T., Theory of solvent effects on molecular electronic spectra. Frequency shifts, *Bull. Chem. Soc. Jpn*., 1965, **30**, 1314–1318.
2. BAKHSHIEV, N.G., Universal intermolecular interactions and their effect on the position of the electronic spectra of molecules in two component solutions, *Opt. Spectrosc*., 1962, **13**, 24–29.
3. BERMACK, J.E., N. HADDJERI, G. DEBONNEL, Effects of the potential antidepressant OPC-14523 [1- [3- [4- (3- chlorophenyl)-1-piperazinyl] propyl]-5-methoxy - 3,4- dihydro -2-quinolinone monomethanesulfonate] a combined σ and 5-HT_{1A} ligand: Modulation of neuronal activity in the dorsal raphe nucleus, *J. Pharmacol. Exp. Theor*., 2004, **310**, 578–583.
4. CLOSCA, VALENTINA, LILIANA MIHAELA IVAN, DANA ORTANSA DOROHOI, Intermolecular interactions in binary and ternary solutions of two cycloimmonium-carboethoxy-anilido-methylids, *Ukr. J. Phys.*, 2014, **59**, 226–232.
5. CRAMER, C.J., *Essentials computational chemistry*, Wiley, Hoboken, N.J., 2004.
6. DOROHOI, DANA ORTANSA, HELENE PARTENIE, The spectroscopy of the cycloimmonium ylides, *J. Molec. Struct*., 1993, **293**, 129–132.
7. FRANCL, M.M., W.J. PIETRO, W.J. HEHRE, J.S. BINKLEY, D.J. DEFREES, J.A. POPLE, M.S. GORDON, Self-consistent molecular orbital methods. A polarization-type basis set for 2nd-row elements, *J. Chem. Phys.*, 1982, **773**, 654–665.
8. FRISCH, M.J., *et al*., Gaussian 09, Revision A.01, Gaussian Inc, Wallingford CT, 2009, http://www.gaussian.com/g_tech/g_ur/m_citation.htm.
9. GEORGESCU, E., C. DRAGHICI, PAULA C. IUHAS, FLORENTINA GEORGESCU, A new approach for the synthesis of benzo[*f*]pyrrolo[1,2-*a*]-quinolines, *Arkivoc*, 2005, **x**, 95–104.
10. GOMHA, S.M., K.M. DAWOOD, Synthesis of novel indolizine, pyrrolo[1,2-*a*] quinoline, and 4,5-dihydrothiophene derivatives *via* nitrogen ylides and their antimicrobial evaluation, *J. Chem. Res*., 2014, **38**, 515–519.
11. HANWELL, M.D., D.E. Curtis, D.C. LONIE, T. VANDERMEERSCH, E. ZUREK, G.R. HUTCHISON, Avogadro: an advanced semantic chemical editor, visualization, and analysis platform, *J. Cheminformat.*, 2012, **4**, 17.
12. HOMOCIANU, MIHAELA, A. AIRINEI, DANA ORTANSA DOROHOI, Solvent effects on the electronic absorption and fluorescence spectra. *J. Adv. Res. Phys*., 2011, **2**, 011105.
13. KIM, K., K.D. JORDAN, Comparison of density functional and MP2 calculations on the water monomer and dimer, *J. Phys. Chem*., 1994, **98**, 10089–10094.
14. KUMAR, S., S. BAWA, S. DRABU, H. GUPTA, L. MACHWAL, R. KUMAR, Synthesis, antidepressant and antifungal evaluation of novel 2-chloro-8-methylquinoline amine derivatives, *Eur. J. Med. Chem*., 2011, **46**, 670–675.
15. MATAGA, N., T. KUBOTA, Molecular interactions and electronic spectra, M. Decker, Inc., NewYork, 1970.
16. NADEJDE, CLAUDIA, DORINA CREANGA, I. HUMELNICU, ELENA FILIP, DANA ORTANSA DOROHOI, Study on the intermolecular interactions in rifampicin ternary solutions – Calculation of microscopic parameters of rifampicin molecules, *J. Mol. Liq*., 2009, **150**, 51–55.
17. Mc RAE, E., Theory of solvent effects on molecular electronic spectra. Frequency shifts, *J. Phys. Chem.*, 1957, **61**, 562–572.
18. ORIGINPRO 7.5 SR0 v7.5714 (B714) from OriginLab Corporation, http://www.OriginLab.com.
19. ROEPE, P.D., The molecular and physiologic basis of quinoline drug resistance in *P. falciparum* malaria, *Future Microbiol*., 2009, **4**, 441–455.
20. SHELKE, S.M., S.H. BHOSALE, Synthesis, antidepressant evaluation and QSAR studies of novel 2-(5H-[1,2,4] triazino [5,6-b] indol-3-ylthio)-N-(substituted phenyl)acetamides, *Bioorg. Med. Chem. Lett*., 2010, **20**, 4661–4664.

21. STEPHENS, P.J., F.J. DEVLIN, C.F. CHABALOWSKI, M.J. FRISCH, Ab initio calculation of vibrational absorption and circular dichroism spectra using Density Functional Force Fields, *J. Phys. Chem*, 1994, **9**,11623–11627.
22. UCHUSKIN, M.G., A.S. PILIPENKO, O.V. SERDYUK, I.V. TRUSHKOV,' A.V. BUTIN, From biomass to medicines. A simple synthesis of indolo [3,2*c*] quinolines, antimalarial alkaloid isocryptolepine, and its derivatives, *Org. Biomol. Chem.*, 2012, **10**, 7262–7265.
23. YOUNG, D.C., Computational chemistry a practical guide for applying techniques to real-world problems, John Wiley & Sons, 2001.
24. ZHANG, G., C.B. MUSGRAVE, Comparison of DFT methods for molecular orbital eigenvalue calculations, *J. Phys. Chem. A*, 2007, **111**, 1554–1561.
25. http://katakago.sakura.ne.jp/cc/moview/d7-3-9/d0002.arc.
26. HYPERCUBE. HyperChem version 8.0.10 Package, Gainesville, FL, USA: Hypercube, 2011.